Climatic Change (2013) 119:825–839
DOI 10.1007/s10584-013-0739-y

Projected shifts of wine regions in response to climate change

M. Moriondo · G. V. Jones · B. Bois · C. Dibari · R. Ferrise · G. Trombi · M. Bindi

Received: 20 June 2012 / Accepted: 4 March 2013 / Published online: 29 March 2013

Abstract This research simulates the impact of climate change on the distribution of the most important European wine regions using a comprehensive suite of spatially informative layers, including bioclimatic indices and water deficit, as predictor variables. More specifically, a machine learning approach (Random Forest, RF) was first calibrated for the present period and applied to future climate conditions as simulated by HadCM3 General Circulation Model (GCM) to predict the possible spatial expansion and/or shift in potential grapevine cultivated area in 2020 and 2050 under A2 and B2 SRES scenarios. Projected changes in climate depicted by the GCM and SRES scenarios results in a progressive warming in all bioclimatic indices as well as increasing water deficit over the European domain, altering the climatic profile of each of the grapevine cultivated areas. The two main responses to these warmer and drier conditions are 1) progressive shifts of existing grapevine cultivated area to the north–northwest of their original ranges, and 2) expansion or contraction of the wine regions due to changes in within region suitability for grapevine cultivation. Wine regions with climatic conditions from the Mediterranean basin today (e.g., the Languedoc, Provence, Côtes Rhône Méridionales, etc.) were shown to potentially shift the most over time. Overall the results show the potential for a dramatic change in the landscape for winegrape production in Europe due to changes in climate.

Electronic supplementary material The online version of this article (doi:10.1007/s10584-013-0739-y) contains supplementary material, which is available to authorized users.

M. Moriondo (✉)
CNR-IBIMET, via G. Caproni 8, 50145 Florence, Italy
e-mail: marco.moriondo@cnr.it

G. V. Jones
Department of Environmental Studies, Southern Oregon University, 101A Taylor Hall, Ashland, OR 97520, USA

B. Bois
Institute of the Vine and Wine "J. Guyot", University of Burgundy, rue Claude Ladrey 1, Dijon Cedex 21078, France

C. Dibari · R. Ferrise · G. Trombi · M. Bindi
Department of Agri-food Production and Environmental Sciences, University of Florence, Piazzale delle Cascine 18, Florence 50144, Italy

1 Introduction

Centuries of experience in viticulture have matched varieties with the environments in which they perform best, resulting in the finest wines associated with geographically distinct viticulture regions in the European countries (Jones et al. 2005a). Over these areas, viticultural regions are confined to specific climatic niches that put them at greater risk from changes in rainfall and temperature that may destabilize the equilibrium between climate, soil and variety, which profoundly influences the production of high quality wines.

Despite the complexity of these interactions, only a few climatic indices have been used as metrics to establish historic and current suitability and identify the potential of a region for wine production in future decades (Fregoni 2003; Jones et al. 2010; Hall and Jones 2010). The majority of bioclimatic indices used in viticulture and wine production are those that typically accumulate heat over the growing season, representing different formulations of growing degree-days such the Huglin Index (HI; Huglin 1978) and the Winkler Index (WI; Amerine and Winkler 1944). As an example, research by Stock et al. (2005) showed that increases of 100–600 units in the HI by 2050 in Europe would result in a latitudinal shift of grapevine cultivation, with new areas on the northern fringes becoming viable, changes in varietal suitability in existing regions, and southern regions becoming too hot to produce high-quality wines. Jones et al. (2005b) also examined numerous locations across Europe finding significant increases in both the WI and HI that showed significant relationships with earlier grapevine phenology and harvest timing. Furthermore, Jones et al. (2005a) demonstrated that simple average growing season temperatures play an important role for quality vintages and that the optimum temperature threshold for ripening is variety dependent. Accordingly, increases in temperature may result in decreased quality for those varieties that are cultivated close to their optimum climatic conditions and, in a warmer climate, varieties may be shifted from their original cultivation areas to match their climatic requirements.

However, these thermal bioclimatic indices alone may not be able to provide a complete climatic description of grape-growing regions and their suitability, further considering that both extreme heat and extreme cold events may be additional factors limiting the production of high quality winegrapes or grapevine cultivation itself (White et al. 2006). As a consequence, future projections of climate in wine regions based on single indices may be partially correct or contradictory because they may not capture the true suitability experienced today. By contrast, better descriptions of the climatic structure and suitability of a wine region may be obtained by a combination of different bioclimatic indices, in some cases including extreme events. For example, Tonietto and Carbonneau (2004) used the combination of three complementary indices, namely the HI, the Dryness Index (DI) and the Cool Night Index (CI) to classify climate stations in wine regions in numerous countries. Kenny and Harrison (1992) developed a Latitude Temperature Index (LTI) in combination with a winter severity constrained thermal index to assess climate suitability of grapes in different areas of Europe. White et al. (2006) combined the WI and extreme event frequencies to highlight possible shifts and expansion/contraction of grapevine areas in the western United States over the next century.

Building on this background, the goals of this research are to examine numerous factors that define the climates and most important characteristics of European wine regions today and then project these characteristics into the 21st century. The results will provide insights into possible shifts, expansion, or contraction in areas suitable for grapevine cultivation due to climate change by considering the specificity of climate-variety in European wine regions. As such, a comprehensive suite of spatially informative layers, including thermal and hydrologic indices, were first exploited to examine the spatial structure, distribution and variability of many of the most well-known European wine regions. These parameters were used as driving variables of

the Random Forest (RF) classification algorithm (Breiman 2001). Once calibrated to current conditions, the RF was used to derive information on the relative importance of the parameters considered in the classification process and to outline possible changes in the cultivated area in grapevines for two different future time slices (2020 and 2050), and for the A2 and B2 SRES emission scenarios (Nakićenović et al. 2000).

The paper has been organized as follows: the methodology section introduces the RF algorithm, presents the spatially informative layers used in the classification, including the current extension of the cultivated area in grapevines and the climate indices used as predictor variables. The RF calibration–validation strategy is also outlined. The results section presents the performance of the classification algorithm and its application for future time slices, describing the effect of a warmer climate on both the expansion/contraction of the entire grapevine cultivated area and the potential shifts of wine regions. Finally, these results are discussed, focusing on the performance of the RF calibration–validation strategy and the different trends in areas viable for grapevine cultivation in the future.

2 Material and methods

2.1 Climatic data

The climate for the present and future periods, were derived from the WorldClim database (Hijmans et al. 2005) which provides average monthly precipitation and temperature values (minimum and maximum temperatures) at a spatial resolution of approximately 1×1 km as well as the relevant Digital Elevation Model (DEM). For the present period, monthly climatology is calculated over the period 1950–2000. Monthly climatic mean temperatures and cumulative rainfall were used to calculate a set of indices to comprehensively describe the climatic structure of European wine regions using a set of bioclimatic indices commonly used in viticulture such as the average minimum temperature of the coldest month (January, T_JAN), the average maximum temperature of the warmest month (July, T_JUL), the Cool Night Index (CI), the Average Growing Season Temperature (AVG_T), three formulations of growing degree-days that are classed into the Winkler, Huglin and the Biologically Effective Degree-Days indices (Gladstones 1992) (WI, HI, and BEDD) and the water deficit index (W_DEF) (Tab. 1 in Electronic Supplementary Material 1).

The DEM was used to characterize the landscape (elevation, slope, and aspect) within the current regions. The pedological properties of the study area (i.e. soil depth and texture), were extracted from the European Soil DataBase (ESDB) (http://eusoils.jrc.ec.europa.eu/) and were used to derive the available water capacity (AWC) that was used for the calculation of Water Deficit index (see Electronic Supplementary Material 2 for details on datasets and 3 for AWC and W_DEF calculation).

Data for future periods are from the simulations of the HadCM3 (Pope et al. 2000) for the A2 and B2 IPCC SRES emission scenarios (Nakićenović et al. 2000), and are referenced to 30-year periods centered on 2020 (average of 2010–2039) and 2050 (average of 2040–2069).

2.2 Grapevine cultivated area

The polygons defining the current grapevine cultivated area over the European domain (including Portugal, Spain, France, Italy and Germany) were derived from the Corine Land Cover database (Bossard et al. 2000), at a spatial resolution of 250×250 m (Electronic Supplementary Material 2 for details). These vector polygons were extracted and gridded to

match the spatial resolution of the climatic dataset (from 250×250 m to 1×1 km) (Fig. 1). Each pixel over the European domain was then assigned to the set of predictor variables to construct an input response/predictor table. The polygons outlining the winegrowing appellations of the most important wine regions were manually digitized from the map published in Carte geographique des vignoble d'Europe 2007 (Editions Benoit, France) (Fig. 1).

2.3 RF classification model

The RF is a classification method that basically consists of an ensemble of decision trees where each tree is generated using a bootstrap sample of the original response/predictor input table. The bootstrap sample, in turn, is randomly split into two subsets, which are used for training (66 %) and for internal testing (33 %, out-of-bag sample, OOB). A classification tree is fit to each bootstrap sample where at each node, a given number of input variables (parameter *mtry*) are randomly chosen and the best split is calculated only within this subset. This parameter is generally set to the square root of the number of input variables.

This procedure reduces the problem of correlated variables because these may be extracted in turn, thus contributing independently to the aggregated tree model. Each tree is fully grown until a final node is reached and then it is used to predict the classes of OOB observations. This procedure is repeated until the desired number of trees is reached (parameter *ntree*).

In the prediction mode, a calibrated RF model consists of an ensemble of classification trees each of which is allowed one vote for the model prediction. The most voted prediction from all of the trees in the random forest becomes the final model prediction.

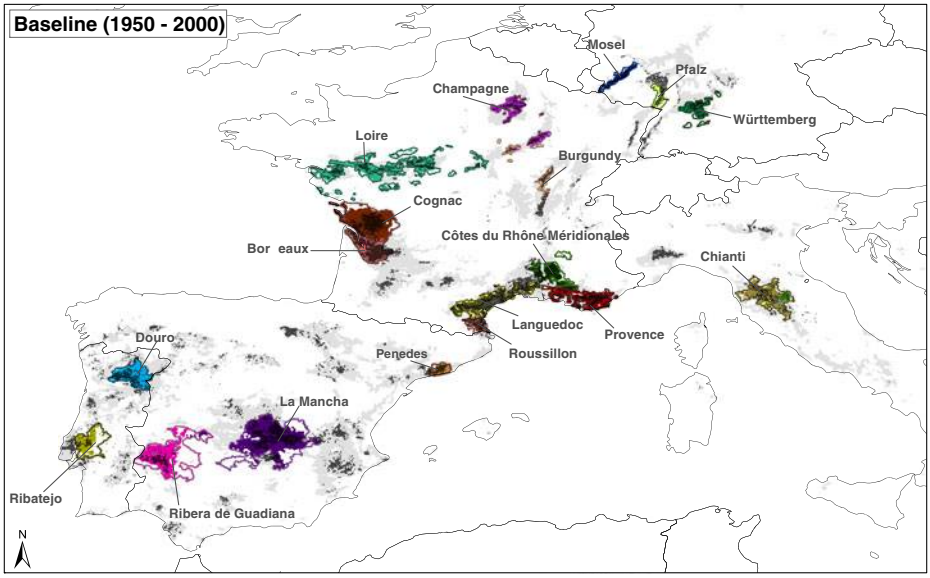

Fig. 1 Reproduction of grapevine cultivated areas and the relevant wine regions for the baseline time period (1950–2000). Wine regions boundaries and the relevant pixels classified by the Random Forest (RF) model are represented with the *same color. Gray pixels* represent areas outside the considered wine regions that were classified as suitable for grapevine cultivation. *Black pixels* represent actual grapevine cultivated areas as obtained by the Corine Land Cover Database

The algorithm includes the computation of the OOB error estimate, which is calculated for each tree over the data split from the corresponding bootstrap sample, and then averaged. Because the OOB observations are not used in the training of the trees, these are essentially cross-validated accuracy estimates. The RF algorithm also provides a measure of variable importance in the modeling, which is obtained by permuting OOB data.

The relationships between individual predictor variables and predicted probabilities of species presence may be additionally investigated by calculating the dependence of the probability of presence on one predictor variable after averaging out the effects of the other predictor variables in the model (partial dependence plot).

2.4 RF model training

The dataset introduced in the previous sections presents two inherent limitations: the extremely large amount of data to be elaborated in the classification process and the very small proportion of pixels belonging to the wine regions over the whole study area. With unbalanced data such as in this analysis, the RF model would tend to overestimate the majority class (i.e. not belonging to that particular wine region), while the algorithm should be preferably trained using a similar amount of test cases (Evans et al. 2011). Because of these potential issues, we split the training of the RF algorithm in two sequential steps. In the first stage we trained the RF to identify the areas suitable for grapevine cultivation, using the wine region layer as a binary response variable (1 = presence, 0 = absence). A sub-sampling procedure of the dataset was tested to find the best compromise between the performance of the model and the size of the input data. In particular, RF was calibrated using 20 different datasets that in turn were sub-sampled from 10 % to 100 % of their original size. Using this procedure, we tested the accuracy of the sub-sampling scheme, i.e. how much do the predictions differ obtained by RF models calibrated with different datasets, and what is the optimum size of the sub-sampling required for an appropriate calibration of the RF?

As a second step, another RF model was trained using a sub-sample corresponding to only the data of the wine regions in order to discriminate amongst different wine regions. This RF algorithm was then applied to those pixels which were classified as part of the grapevine cultivated area to predict the relevant wine region (see Electronic Supplementary Material 4 for details).

2.4.1 Accuracy statistic

When predicting the presence/absence, the RF model generates non-dichotomous scores on an ordinal scale between 0 and 1. Its performance is then evaluated by applying a certain threshold to transform the scores into a set of binary, presence/absence predictions to be compared to observed data. In this research, the possible thresholds to be applied were scaled between 0 and 1 with a step of 0.1 and for each threshold the relevant number of true positive (a), false positive (b), false negative (c) and true negative (d) cases predicted by the model were recorded. These indices were then combined in the accuracy metric proposed by Allouche et al. (2006) termed the true skill statistic (TSS):

$$TSS = \frac{ad - bc}{(a + c)(b + d)} \tag{1}$$

TSS ranges from −1 to +1, where +1 indicates perfect agreement and values of zero or less indicate a performance no better than random.

Where the classification produces multiple classes, the RF model provides for each pixel a probability, summed to 1, which belongs to each of the wine regions examined. The predicted class is therefore the one that has a greater probability in the suite of chosen wine regions.

3 Results

3.1 Climatic structure of wine regions

The subset of European winegrowing regions analyzed exhibits a large diversity of terrain and climate characteristics. On average, median elevation ranges from 47 m asl (Bordeaux) to 689 m asl (La Mancha) while the most frequent aspects in the wine regions span from SSE to SSW (Table 1). The spatial structure of the climatic indices shows a clear north–south pattern, with hot and dry conditions present along the Mediterranean basin while cool conditions are mainly observed in the inner continental areas. The AVG_T ranges from 13.9 °C (Mosel) to 20.9 °C (Ribera de Guadiana), which corresponds to cool to hot climate-maturity conditions, respectively, as defined by Jones et al. (2005a). The heat accumulation indices WI, HI, and BEDD, produced broadly similar results, with the lowest values generally observed in the Mosel, Champagne and Pfalz and the highest in Ribera de Guadiana and La Mancha. The minimum temperature in January (T_JAN) ranged from −2.2 °C in Württemberg to 7.8 °C in Ribatejo while the maximum temperature in July (T_JUL) was observed in Ribera de Guadiana (34 °C) and the lowest in the Mosel (22.9 °C). The Mosel, Württemberg, and Pfalz exhibited the lowest CI values of the wine regions (<10 °C), while Ribera de Guadiana, Ribatejo, and Penedes has the highest CI values (15.9–17.3 °C). For W_DEF, Württemberg and Bourgogne showed the lowest water deficits (<100 mm) while La Mancha and Ribera de Guadiana had deficits of 390 mm and 462 mm, respectively (Table 1). See Electronic Supplementary Material 5 for further analysis.

3.2 Model calibration and validation

The results of the calibration were homogeneous for all the datasets and generally indicated that the best performances were obtained starting from 80 % of the dataset with a threshold higher than 0.7 maximizing the TSS error index (0.92) (Fig. 1 in Electronic Supplementary Material 6). This result was confirmed by the analysis of the OOB errors (i.e., the internal error of the calibration procedure), which decreased as the training set increased up to 60 % and then remained nearly unchanged thereafter (Fig. 2 in Electronic Supplementary Material 6). Overall these results indicate the efficiency of the sub-sampling procedure to the extent that the performances of the RF model were high (TSS=0.92) and not affected by the sub-sample used. Additionally, training datasets even larger than those used in this study would not reduce the prediction error, indicating that the sample size is adequate to provide the best performances in the training phase.

Given these results, we calibrated the RF model using a single dataset, which was then used to classify the entire European domain used in this study. This dataset was previously randomly split into 80 % and 20 % of the total test cases, which were used to calibrate and validate the RF model, respectively. The calibration phase resulted in an OOB of 6.12 % with a threshold maximizing TSS higher than 0.7 (TSS=0.93). The calibrated RF model was then applied on the validation subset, resulting in a similar TSS accuracy (0.89) when using

Table 1 Climatic and terrain features of the 18 wine regions. Longitude and latitude are given as the centroid of the wine region. Surface represents the areas relevant to each wine region, while elevation is the median and standard deviation of the wine region and aspect is the predominant direction of the landscapes in the regions. N° pixels refers to the number of pixels indicated by the Corine Land Cover as belonging to grapevine cultivation in each region. HI and WI are the Huglin and Winkler indices respectively, BEDD is the Biologically Effective Degree-Days, AVG_T is the average temperature during the season (Apr–Oct), CI is the Cool Night Index, T_JAN and T_JUL are minimum temperature of the coldest and maximum temperatures of warmest month, respectively, and W_DEF is the water deficit calculated during the growing season

Wine region	Lon E (°)	Lat N (°)	Elevation (m asl)	Aspect	Surface (Km^2)	Pixels (n°)	HI (°C)	BEDD (°C)	AVG_T (°C)	CI (°C)	WI (°C)	T_JUL (°C)	T_JAN (°C)	W_DEF (mm)
Bordeaux	0.43	48.8	47±27	SSE	5348.4	2414	1850±89	1339±53	16.9±0.5	12.1±0.6	1382±104	25.8±0.6	1.5±0.7	113±45
Bourgogne	4.33	47.4	269±55	SSE	2049.3	443	1610±126	1100±84	15.1±0.7	11±0.7	1113±134	24.7±0.8	−1±0.6	97±38
Champagne	4.28	48.6	173±55	SSE	3133.5	671	1454±59	912±44	14.1±0.4	10±0.2	919±60	23.7±0.5	−1.2±0.5	114±19
Chianti	11.33	43.52	221±131	SSW	7246.6	482	2162±104	1484±80	18.2±0.6	14.2±0.9	1766±129	29.1±0.7	1.8±1.1	191±38
Cognac	0.4	45.62	54±29	S	10916.3	1713	1774±71	1295±36	16.3±0.6	12.2±0.5	1333±73	25.3±0.7	1.8±0.4	123±28
Côtes Rhône M.	5.2	44.13	181±102	SSW	4525.1	2332	2021±64	1391±53	17.3±0.4	12.9±0.4	1563±54	28.2±0.6	0.4±0.5	212±13
Douro	−7.28	41.23	441±149	SSE	5502.6	1243	2125±87	1468±59	17.9±0.6	13±0.7	1677±113	29.1±0.5	2.7±0.7	258±39
La Mancha	−3.37	39.57	689±48	SSW	22923.0	4312	2417±135	1472±77	18.9±0.8	13.5±0.7	1905±158	32.8±0.8	0.8±0.8	390±64
Languedoc	3.13	43.43	98±79	SSE	5439.9	6147	2144±164	1510±108	18.2±0.9	14.3±0.8	1762±184	28.5±0.9	2±0.9	259±47
Loire	−0.37	47.17	78±51	S	12531.6	1158	1606±40	1138±42	15.1±0.5	11.2±0.5	1137±35	24.4±0.7	1±0.5	164±16
Mosel	7.1	50.05	207±40	S	1418.2	357	1381±36	881±21	13.9±0.4	9.8±0.3	887±29	22.9±0.4	−1.3±0.5	102±5
Penedes	1.72	41.38	236±101	SSE	1698.8	577	2138±54	1600±43	19.2±0.5	17.3±0.2	1959±47	27.1±0.3	5.1±0.2	261±13
Pfalz	8.13	49.4	170±45	E	1488.4	459	1518±44	980±34	14.6±0.3	9.9±0.2	986±42	24±0.5	−2±0.4	107±19
Provence	5.87	43.43	196±114	S	5542.6	1061	1955±50	1464±47	17.7±0.4	14.4±0.5	1644±43	26.8±0.6	2.5±0.8	265±20
Ribatejo	−8.47	39.22	63±54	SSW	5948.2	335	2202±57	1707±39	19.3±0.3	16.3±0.3	2010±67	27.3±0.3	7.8±0.4	373±12
Ribera de Guadiana	−6.12	38.73	319±82	SSW	15802.5	823	2727±82	1695±71	20.9±0.5	15.9±0.4	2309±71	34±0.4	3.9±0.4	462±20
Roussillon	2.78	42.03	134±122	E	1633.8	923	2188±111	1567±29	19±0.5	15.8±0.6	1899±100	28.2±1.1	3.4±0.5	285±32
Württemberg	9.1	48.8	263±52	SSW	2577.7	219	1539±145	1003±84	14.7±0.8	9.8±0.9	1008±161	23.8±0.8	−2.2±0.7	76±14

the same threshold (i.e. >0.7). The robust and coherently calibrated RF model was then applied to the predictor variables calculated for the baseline and for the future time slices (2020 and 2050) to derive the relevant grapevine cultivated area.

The RF model calibrated to discriminate the 18 wine regions showed nearly complete classification accuracy with OOB errors ranging from 0.2 (La Mancha) to 2.9 % (Roussillon) with an overall OOB error of 1.1 % (data not shown). This result was confirmed using the validation dataset which resulted in an overall error of 1.8 %. When the RF model was applied over the entire grapevine cultivated area (as simulated for the present period) it generally over-predicted the area of the studied wine regions even though they were seldom misclassified (Fig. 1).

3.3 Predictor importance and predictability

The parameters W_DEF, HI, and T_JAN were the most important in predicting the presence of vineyards, while T_JUL and AVG_T had the lowest prediction potential.

Despite the great variability in the climates of the grapevine cultivated areas, the analysis of the predictability of presence (partial plot) showed some common trends over the study area. More specifically, climatic indices define the presence of grapevine areas approximating a bell-shaped curve: the predictability of grapevine presence in response to increasing values of the climatic index generally increases up to a maximum and then drops again (Fig. 3 in Electronic Supplementary Material 4).

T_JUL, W_DEF and CI were the variables having the greater importance for classification of the single wine regions (data not shown) while the partial plots for each wine region further indicated that there typically exists a climatic gradient in grapevine suitability (Fig. 4–10 in Electronic Supplementary Material 4).

3.4 Impact of climate change on wine areas

Future climatic change, as projected by HadCM3 under A2 and B2 emission scenarios, resulted in progressively warmer and drier conditions over the study area. This trend is reflected by a concomitant increase in all temperature-related indices and the water deficit over the domain which alters the climatic structure of the grapevine cultivated areas (Tab. 1, 2 in Electronic Supplementary Material 7).

The intensity of climatic change followed a clear latitudinal pattern, with southern wine regions recording a dramatic increase in HI, W_DEF, T_JUL and T_JAN, while similar trends were observed in the north, but at lower rates. This asymmetric pattern resulted in a progressive northern shift of grapevine cultivation from its original range, with some differences between A2 and B2 scenarios (Fig. 2). The impact was particularly evident in the southern regions of the Mediterranean basin, where the combination of climatic factors that have helped defined the wine production suitability of these regions in the present period, were found to gradually disappear starting in 2020. Many wine producing regions over the Iberian Peninsula and France also are projected to lose suitability in inland areas, shifting toward the Atlantic coast, which remains a local *refugium* through 2050. In Germany, grapevine cultivation is predicted to be extended along the north-eastern section of the country, reaching the northern fringes of the region by 2050.

Given the changes in climate structure over the domain, existing wine regions where found to expand, contract and/or shift depending on the local changes in the climate suitability for grapevine cultivation (Table 2). Overall, two different general trends were observed. The main response was that some of the wine regions found similar present day

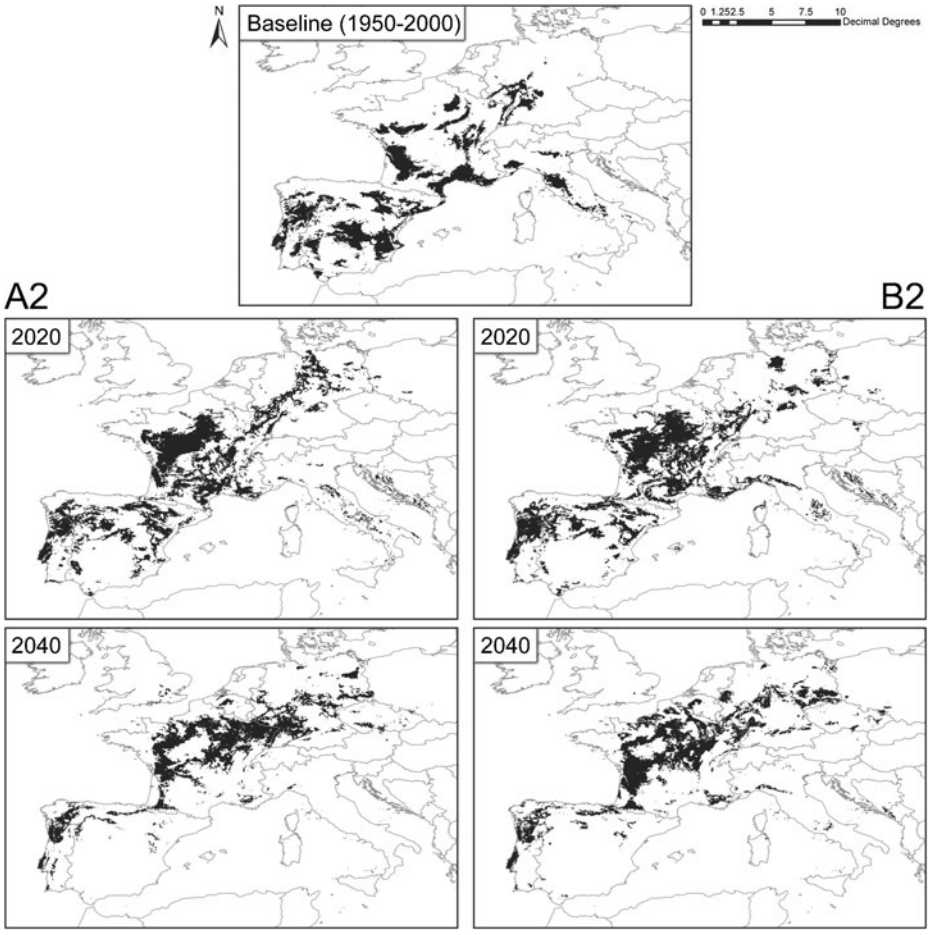

Fig. 2 Predicted grapevine cultivated area for the baseline (1950–2000) and the future time slices 2020 and 2050 in A2 and B2 scenarios

climatic conditions relatively close to their original location but showed shifts to higher elevation (Fig. 3 in Electronic Supplementary Material 6). These changes were typically associated with decreases in area. This is the case for the Chianti area which, in 2020, while remaining approximately in the same region as it is presently, moved from an average elevation of 211 m asl to 450 and 455 m asl (A2 and B2) with a reduction of 83 % and 77 % of its area simulated for the present period, respectively. The same trend is reflected in 2050, where a slight northern shift of the region (+1.5° Lat N in A2; +1.4 Lat N in B2) is still associated with an increase in the average elevation (+356 m and 338 m in A2 and B2) and with a large reduction of its original extension (−61.5 % and −97.7 % in A2 and B2). The same shifts occur in La Mancha in 2020 and 2050 (Table 2) where a progressive shift to higher elevation, close to its original range (e.g. in A2 the area best suited for La Mancha shifted northward by 0.9° to 1.6° Lat N), was accompanied by a large decrease in area in both A2 and B2. The other common response is found in wine regions such as Côtes Rhône Méridionales, Cognac, Loire, Mosel and Pfalz where each found their present day climatic conditions further north away from their original range, but at lower elevations. These types

Table 2 Change in wine region area, elevation, and latitudinal position in response to a warmer climate in emission scenarios A2 and B2 for the 2020 and 2050 time slices ([a] indicates the absence of the wine region). Data for the baseline are calculated according the predicted grapevine cultivated area and the relevant wine region distribution simulated for that period. Area is expressed in square kilometers, elevation in meters and position in degree latitude North

Wine region	Area	Elevation	Position	A2						B2					
				Change in area (%)		Change in elevation (m)		Change in position (°)		Change in area (%)		Change in elevation (m)		Change in position (°)	
				2020	2050	2020	2050	2020	2050	2020	2050	2020	2050	2020	2050
Bordeaux	22995	79.4	44.6	−57.7	−62.6	−17.3	18.0	0.4	3.2	−63.9	−37.6	59.3	29.0	0.9	3.6
Bourgogne	8120	276.9	46.8	−74.5	−70.6	258.8	105.8	−0.7	3.2	−43.9	−50.6	−18.5	−18.0	2.9	3.6
Champagne	9381	180.0	48.8	−8.1	−99.8	−90.7	164.4	3.4	2.4	−97.5	−96.6	19.3	−41.8	2.1	4.0
Chianti	13345	210.7	43.8	−83.4	−61.5	242.3	145	−0.2	1.5	−77.1	−97.7	244.8	127.3	−0.5	1.4
Cognac	12354	63.2	45.6	69.3	49.7	57.3	75.1	1.3	3.9	60.2	89.2	58.6	27.8	1.6	4.0
Côtes Rhône M.	16607	276.4	43.6	67.6	171.0	40.5	−56.2	1.9	4.7	84.6	133.0	34.6	5.6	3.3	3.9
Douro	27694	553.3	41.0	−46.9	−61.0	20.6	−193.9	0.7	4.0	−40.1	107.8	22.1	−348.8	0.5	4.8
La Mancha	39234	688.5	39.4	−43.3	−94.1	91.6	179.1	0.9	1.5	−45.1	−97.7	107.5	125.2	1.6	1.0
Languedoc	27059	178.7	43.4	−86.0	−14.6	95.8	73.0	−0.4	2.8	−80.7	−83.8	223.5	−8.6	0.0	1.2
Loire	16528	95.5	47.2	137.1	−80.2	3.7	56.6	0.2	2.0	74.3	−36.0	31.1	28.2	0.6	2.7
Mosel	2118	194.4	49.9	8.8	[a]	−86.4	[a]	2.5	[a]	[a]	[a]	[a]	[a]	[a]	[a]
Penedes	5244	195.6	41.0	−93.2	−99.9	−105.6	179.7	0.1	1.5	−89.4	−98.1	59.6	117.5	0.7	1.8
Pfalz	6491	172.8	49.8	72.4	−27.2	20.0	246.9	1.2	0.8	87.0	−85.0	−8.9	177.1	1.9	1.0
Provence	18819	404.6	42.4	211.6	216.4	−221.8	−273.7	4.3	6.3	197.3	67.8	−246.7	−313.9	4.6	5.3
Ribatejo	13847	79.9	38.8	7.6	−58.0	14.6	42.6	0.6	1.0	3.6	−31.9	20.0	54.1	0.7	1.1
Ribera de G.	13829	312.6	38.5	−78.8	−99.1	85.3	−137.7	0.4	1.1	−94.5	−99.5	142.9	300.5	0.5	−0.6
Roussillon	5208	214.2	42.6	−94.9	[a]	311.5	[a]	−0.8	[a]	−78.2	−98.0	73.0	−102.5	1.1	1.2
Württemberg	5813	244.4	49.1	−44.5	−47.3	267.9	212.8	−2.2	0.0	−66.4	−16.3	335.6	139.3	−2.3	1.0

of shifts typically came with increases in their overall area but with different magnitudes depending on the time period and emission scenario.

4 Discussion

4.1 Model calibration

The proposed calibration strategy demonstrated that it was not affected by the sampling procedure and the results further indicated that the size of the dataset used for the training phase ensured the highest accuracy performances of the RF model. In fact, the OOB error and TSS were minimized when using 70 % and 80 % of the original dataset.

The RF model calibrated to predict grapevine cultivated areas indicated that water deficit (W_DEF) was the most important variable in the classification process, which is likely related to the fact that this index combines numerous factors such as day length, average temperature and accumulated rainfall during the growing season, soil depth and texture (Gaál et al. 2012). January minimum temperatures (T_JAN), which yields a score slightly lower than W_DEF, gives additional information to the model about latitudinal and elevation constraints to grapevine cultivation due to extreme cold climatic limits. The Huglin Index (HI) was the most important heat accumulation index (better than WI and BEDD) and this may be related to additional information included in this index such as the mean day length in relation to the latitude and the fact that the HI weights daytime temperatures more than the other two indices. Conversely the average growing season temperatures (AVG_T) did not significantly influence the region's climate classification. While AVG_T is functionally the same as growing degree-days and highly correlated to HI, WI, and BEDD, either explanatory redundancy or the lack of temperature thresholds for grapevine growth may limit its usefulness in this model.

For all the considered parameters, a partial plot analysis shows evidence of the presence of an optimum value corresponding to the higher probability in detecting grapevine areas (see Fig. 3 in Electronic Supplementary Material 4). In particular, for T_JAN, which has a high score for the classification process, the peak is centered over 1.9 °C and, just a few degrees more or less around the optimum, the predictability drops off sharply. This indicates that the presence of grapevines is both limited by its winter cold tolerance as well as by its winter chilling requirements. This tight range of temperatures may have significant implications in a warmer climate. Grapevine cold tolerance is generally acknowledged as one of the main factors limiting the cultivation poleward. On the other hand, the result shows that T_JAN above a threshold was a limit for grapevine cultivation and this may be likely related to an inadequate exposure to chilling temperatures that can lead to patchy or delayed bud break, causing heterogeneous phenological development later in the season (Lavee and May 1997). This may result in significant economic and viticultural problems (Moriondo et al. 2011), thus limiting grapevine cultivation in those areas where mild winter temperatures does not allow a complete fulfillment of chilling requirements.

In the second step, the RF model was trained to discriminate the different wine regions by sub-sampling from the original dataset the climate and topographical features of 18 of the most important wine producing areas in Europe. The large differences in the combination of climatic and topographical factors between these areas resulted in a nearly complete classification accuracy for the selected wine regions. This supports the notion that grapevine

varieties were spatially selected to match the environmental conditions where they performed better, resulting in the definition of wine regions as a unique combination of climatic factors, which define highly specialized ecological niches. Interestingly T_JUL and CI, which did not perform well in classifying the presence/absence of grapevine cultivation areas, had greater informative degree for wine region discrimination (along with W_DEF). While T_JUL may be particularly related to the tolerance of grapevine varieties to heat stress, the importance of CI and W_DEF may be more related to the different qualitative potentials of different wine regions, partially reflecting the findings of Tonietto and Carbonneau (2004), which used CI and W_DEF and HI in a Multicriteria approach to classifying a collection of wine regions worldwide.

The RF model, when applied over the European domain, resulted in a general over-prediction of the areas suitable for each region. It should be noted that the RF model rarely misclassified pixels between the different wine regions. This is coherent with the results obtained during the training stage and indicates the robustness of the RF model in discriminating the different wine regions. The over-prediction of grapevine cultivated area in the present period would be expected since the RF model, once calibrated, may classify areas which may potentially be used for grapevine cultivation but, for reasons other than climatic conditions (e.g., forested or urban areas, etc.), they are not.

Furthermore, the winegrowing region boundaries cover areas substantially larger than the actual vineyards used to calibrate the RF model and the results of our classification are in most cases included within or just surrounding these boundaries, providing indirect proof of the robustness of the calibration.

4.2 Impact of climate change

The HadCM3 model data used in this research simulates a progressively warmer and drier climate which exhibits a latitudinal gradient with higher absolute increases observed over the Mediterranean regions for all of the indices used in this analysis, while a lower increase was observed in the northern regions (Electronic Supplementary Material 7). Similar results for Europe have been found by Malheiro et al. (2010) using a wider range of climate models (IPCC-SRES ensemble simulations) over the entire 21st century. Santos et al. (2012) show that large scale warming has occurred over Europe already (1950–2009) and Jones et al. (2005a) observed that this trend is similar across many wine regions worldwide over the last 50 years. These changes have been found to affect fruit composition with typically higher sugar levels and lower acidity as observed in Alsace (Duchêne and Schneider 2005), the Mosel (Urhausen et al. 2011), Australia (Godden and Gishen 2005) and others. Given that the trends in climate have been largely viewed to have had a general beneficial effect for the quality of wine worldwide (Shultz and Jones 2010), the perceived risk of future climate change in the viticulture and wine production sector is not as high as it should be (Jones and Webb 2010).

The progressive increase in temperature and dryness as simulated for the future periods in this research outlines a potentially radical change in the area that is suitable for cultivating grapevines. The results reveal both positive and negative impacts for viticulture over Europe. While new areas are predicted to become viable for grapevine cultivation, many wine regions will likely find their present day climatic conditions shifted from their original location. In accordance with previous studies (Kenny and Harrison 1992; Stock et al. 2005), areas that are potentially suitable to the cultivation of grapevines gradually shifted northwards due to the combined effect of progressively warmer and drier conditions during the growing season.

However, many of the wine regions examined in this study were also predicted to see shifts in their present day climate zones to higher elevations in the same general area, while others showed significant latitudinal shifts. Some of these latitudinal shifts resulted in areas more commonly suitable for typical Mediterranean wine regions today (e.g., Provence and Languedoc) substantially further poleward, while wine regions originally located in very hot regions, progressively disappeared (Table 2).

Possible shifts in wine regions have been predicted by Jones et al. (2005a) relying on the relationships between AVG_T and wine quality. Our results support and improve this earlier work, to the extent that the potential for grapevine cultivation of a wine area was not related to a single climate parameter or index but to an ensemble of viticultural suitability indices. This approach helped capture the complex climate and landscape structure of wine regions in the present period and was able to identify the geographical areas wine regions may find similar climates in future periods. Analysis of specific climate types and their change in geographical location reveals that this trend has already been observed over Europe in the last 15 years and that some 8 % of its total area was affected by this shift with a significant increase of the area with maritime temperate climates, which replaced mainly the continental temperate climate zones (Fraederick et al. 2001). The simulated climate change in this research supports the notion of expansion of wine region climates, such as those found in Provence and Languedoc today, northwards but more important is the fact that this shift was made possible by the flexibility of these regions in terms of climate requirements. This is evident when analyzing the smoothed-kernel curve distribution of climate indices over these areas (Fig. 2 in Electronic Supplementary Material 5). The larger spatial variability of the main predictor variables ensures the larger adaptability of these regions to new climate conditions.

5 Conclusion

Today's viticultural regions are located in relatively narrow geographical areas between 30° to 50°N and 30° to 40°S with growing season climates that have average temperatures between 12 and 22 °C (Shultz and Jones 2010). Given the inherent climate sensitivity of grapevines, suitable zones for their cultivation are very susceptible to small changes in climate. History has shown this to be the case with grapevine cultivated areas in Europe expanding or contracting driven by changes in climate over the last two millennia (Shultz and Jones 2010). The impacts of future changes in climate on viticultural suitability over Europe and other growing regions worldwide is therefore an important research focus (Jones and Webb 2010). This research has examined potential future changes in European viticulture through a novel ecosystem modeling approach that defines the climate and landscape characteristics of existing regions and then models future changes in these characteristics. Using high resolution climate grids for the HadCM3 model for 2020 and 2050 under the A2 and B2 emission scenarios, the results indicate progressively warmer and drier climate conditions over Europe. As a consequence, wine region climate suitability was shown to shift upward in elevation and/or poleward, while southern regions are projected to become progressively unsuitable for cultivation because of increasing temperatures and water deficit; exceeding the known limits tolerated by grapevine cultivation today.

While this research did not incorporate adaptation options in the RF model, Diffenbaugh et al. (2011) show that the design and implementation of effective climate change adaptation activities can dramatically reduce the impacts. Duchêne and Schneider (2005) stress the

importance of better matches between cultivars and rootstocks that provide enhanced buffers from environmental stresses. In the vineyard numerous initial planting decisions (e.g., row orientation), vine management (e.g., trellising, pruning, etc.), and infrastructure management (e.g., irrigation) have the potential to provide adaptive capacity (Keller 2010). However, more research is needed to understand how adaptive mechanisms might lower risk or impact, so that they can be better implemented in modeling efforts such as this work.

Acknowledgments This research was supported by the Commission of EU (Project MEDIATION, project no. 244012). The authors would like to gratefully acknowledge the constructive comments provided by the two anonymous referees.

References

Allouche O, Tsoar A, Kadmon R (2006) Assessing the accuracy of species distribution models: prevalence, kappa and the true skill statistic (TSS). J Appl Ecol 43:1223–1232

Amerine MA, Winkler AJ (1944) Composition and quality of musts and wines of California grapes. Hilgardia 15:493–673

Bossard M, Feranec J, Otahel J (2000) Corine land cover technical guide — Addendum 2000. http://terrestrial.eionet.europa.eu/. EEA Technical report No 40. Copenhagen (EEA)

Breiman L (2001) Random forests. Mach Learn 45:5–32

Diffenbaugh NS, White MA, Jones GV, Ashfaq M (2011) Climate adaptation wedges: a case study of premium wine in the western United States. Environ Res Lett 6:024024. doi:10.1088/1748-9326/6/2/024024

Duchêne E, Schneider C (2005) Grapevine and climatic changes: a glance at the situation in Alsace. Agron Sustain Dev 25:93–99

Evans JS, Murphy MA, Holden ZA, Cushman SA (2011) Modeling species distribution and change using random forest. In: Drew CA et al (eds) Predictive species and habitat modeling in landscape ecology: concepts and applications. doi:10.1007/978-1-4419-7390-0_8, Springer Science+Business Media, LLC 2011

Fraederick K, Gerstengarbe FW, Werner PC (2001) Climate shift during the last century. Clim Chang 50:405–417

Fregoni M (2003) L'indice bioclimatico di qualitá Fregoni. In: Fregoni M et al (eds) Terroir, Zonazione Viticoltura. Phytoline, Piacenza, pp 115–127

Gaál M, Moriondo M, Bindi M (2012) Modelling the impact of climate change on the Hungarian wine regions using random forest. Appl Ecol Environ Res 10:121–140

Gladstones J (1992) Viticulture and environment. Winetitles, Adelaide

Godden P, Gishen M (2005) Trends in the composition of Australian wine. Aust N Z Wine Ind J 20:21–46

Hall A, Jones GV (2010) Spatial analysis of climate in winegrape-growing regions in Australia. Aust J Grape Wine Res 16:389–404

Hijmans RJ, Cameron SE, Parra JL, Jones PG, Jarvis A (2005) Very high resolution interpolated climate surfaces for global land areas. Int J Climatol 25:1965–1978

Huglin P (1978) Nouveau mode d'évaluation des possibilités héliothermiques d'un milieu viticole. C R Acad Agric France 1117–1126

Jones GV, Webb LB (2010) Climate change, viticulture, and wine: challenges and opportunities. J Wine Res 21:103–106

Jones GV, White MA, Cooper OR, Storchmann K (2005a) Climate change and global wine quality. Clim Chang 73:319–343. doi:10.1007/s10584-005-4704-2

Jones GV, Duchene E, Tomasi D, Yuste J, Braslavksa O, Schultz H, Martinez C, Boso S, Langellier F, Perruchot C, Guimberteau G (2005b) Changes in European winegrape phenology and relationships with climate. GESCO 2005

Jones GV, Duff AA, Hall A, Myers JW (2010) Spatial analysis of climate in winegrape growing regions in the western United States. Am J Enol Vitic 61:313–326

Keller M (2010) Managing grapevines to optimize fruit development in a challenging environment: a climate change primer for viticulturists. Aust J Grape Wine Res 16:56–69. doi:10.1111/j.1755-0238.2009.00077.x

Kenny GJ, Harrison PA (1992) The effects of climate variability and change on grape suitability in Europe. J Wine Res 3:163–183
Lavee S, May P (1997) Dormancy of grapevine buds—facts and speculation. Aust J Grape Wine Res 3:31–46
Malheiro AC, Santos JA, Fraga H, Pinto JG (2010) Climate change scenarios applied to viticultural zoning in Europe. Clim Res 43:163–177
Moriondo M, Bindi M, Fagarazzi C, Ferrise R, Trombi G (2011) Framework for high-resolution climate change impact assessment on grapevines at a regional scale. Reg Environ Change 11:553–567
Nakićenović N et al (2000) Special report on emissions scenarios: a special report of Working Group III of the Intergovernmental Panel on Climate Change. Cambridge University Press, Cambridge, 599 pp
Pope VD, Gallani ML, Rowntree PR, Stratton RA (2000) The impact of new physical parameterizations in the Hadley Centre climate model — HadAM3. Clim Dyn 16:123–146
Santos JA, Malheiro AC, Pinto JG, Jones GV (2012) Macroclimate and viticultural zoning in Europe: observed trends and atmospheric forcing. Clim Res 51:89–103
Shultz HR, Jones GV (2010) Climate induced historic and future changes in viticulture. J Wine Res 21:137–145
Stock M, Gerstengarbe FW, Kartshall T, Werner PC (2005) Reliability of climate change impact assessment for viticulture. Proc. VII IS on Grapevine (Ed. LE Williams). Acta Hort 689, ISHS pp 29–39
Tonietto J, Carbonneau A (2004) A multicriteria climatic classification system for grape-growing regions worldwide. Agric For Meteorol 124:81–97
Urhausen S, Brienen S, Kapala A, Simmer C (2011) Climatic conditions and their impact on viticulture in the Upper Moselle region. Clim Chang 109:349–373
White MA, Diffenbaugh NS, Jones GV, Pal JS, Giorgi F (2006) Extreme heat reduces and shifts United States premium wine production in the 21st century. Proc Natl Acad Sci U S A 103(30):11217–11222